JACS
JOURNAL OF THE AMERICAN CHEMICAL SOCIETY
pubs.acs.org/JACS
Article

B/N-Doped *p*-Arylenevinylene Chromophores: Synthesis, Properties, and Microcrystal Electron Crystallographic Study

Hua Lu, Takayuki Nakamuro, Keitaro Yamashita, Haruaki Yanagisawa, Osamu Nureki, Masahide Kikkawa, Han Gao, Jiangwei Tian, Rui Shang,* and Eiichi Nakamura*

Cite This: *J. Am. Chem. Soc.* 2020, 142, 18990−18996
Read Online
ACCESS | Metrics & More | Article Recommendations | Supporting Information

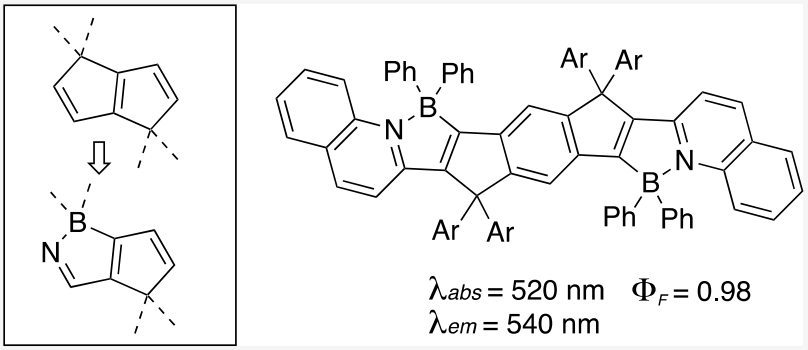

ABSTRACT: Linearly conjugated systems have long served as an archetype of conjugated materials, but suffer from two intrinsic structural problems: potential instability due to intermolecular interactions and the flexibility of the C−C bonds connecting C═C bonds. Efforts to solve these problems have included the insertion of aromatic units as a part of the conjugation and the introduction of carbon bridges to stop the bond rotation. We report here B/N-doped *p*-arylenevinylene chromophores synthesized through the incorporation of a cyclopenta[*c*][1,2]azaborole framework as a part of the conjugated system. The ring strain intrinsic to this new skeleton both flattens and rigidifies the conjugation, and the B^-−N^+ dative bond is much easier to form than a C−C bond, which simplifies the synthetic design. The B−N dative bond also reduces the HOMO−LUMO gap, thereby causing a significant redshift of the absorption and emission compared with their all-carbon congeners while retaining high photostability and high fluorescence quantum yield in both solution and film states. A doubly B/N-doped compound showed emission peaks at 540 nm with a small Stokes shift of 20 nm and a fluorescence quantum yield of 98%. The molecules serve as excellent lipophilic fluorescent dyes for live-cell imaging, showing a higher photostability than that of commercially available BODIPY-based dyes.

1. INTRODUCTION

Linearly conjugated systems, first discovered in a form of polyacetylene in the 1970s, are receiving ever-increasing attention in numerous applications.[1,2] Two intrinsic structural problems remain: potential instability due to intermolecular interactions and flexibility of the C−C bonds connecting the C═C bonds. Insertion of aromatic units into the polyacetylene system (e.g., poly- phenylenevinylenes) has successfully addressed the first problem.[3] Of the strategies to cope with the second problem, the one using carbon-bridged oligophenylenevinylenes (COPVs, Figure 1a) is the most recent, where the large strain of the built-in 1,4-dihydropentalene framework flattens the structure and kinetically stabilizes the molecule (Figure 1a, purple).[4,5] The aryl groups installed on the carbon bridges reduce intermolecular interactions. Together with its spiro variant,[6] the COPV class of molecules has found use in molecular wires and solid-state lasers.[7−9] The synthesis, however, requires many steps, in particular, the synthesis of compounds emitting at a long wavelength (e.g., **COPV6** emitting at 536 nm requires 10 synthetic steps of overall 3.4% yield).[4b] To address this issue, we propose here a new core structure, 1,4-dihydrocyclopenta[*c*][1,2]azaborole (blue) (Figure 1b) containing a B^-−N^+ dative bond, which is a much easier bond to form than a C−C bond.[10−13] Reported below is a new class of linearly conjugated molecules, B/N-doped *p*-arylenevinylenes (Figure 1c), which emit blue to yellow light with fluorescence quantum yield (FLQY) of >95% in solution and 56−100% in a film state with photostability as high as COPVs. The B^-−N^+ bond achieved in the last step of the synthesis not only increases the synthetic efficiency and flexibility but also reduces the band gap, which enables even a

Received: September 28, 2020
Published: October 22, 2020

https://dx.doi.org/10.1021/jacs.0c10337
J. Am. Chem. Soc. 2020, 142, 18990−18996

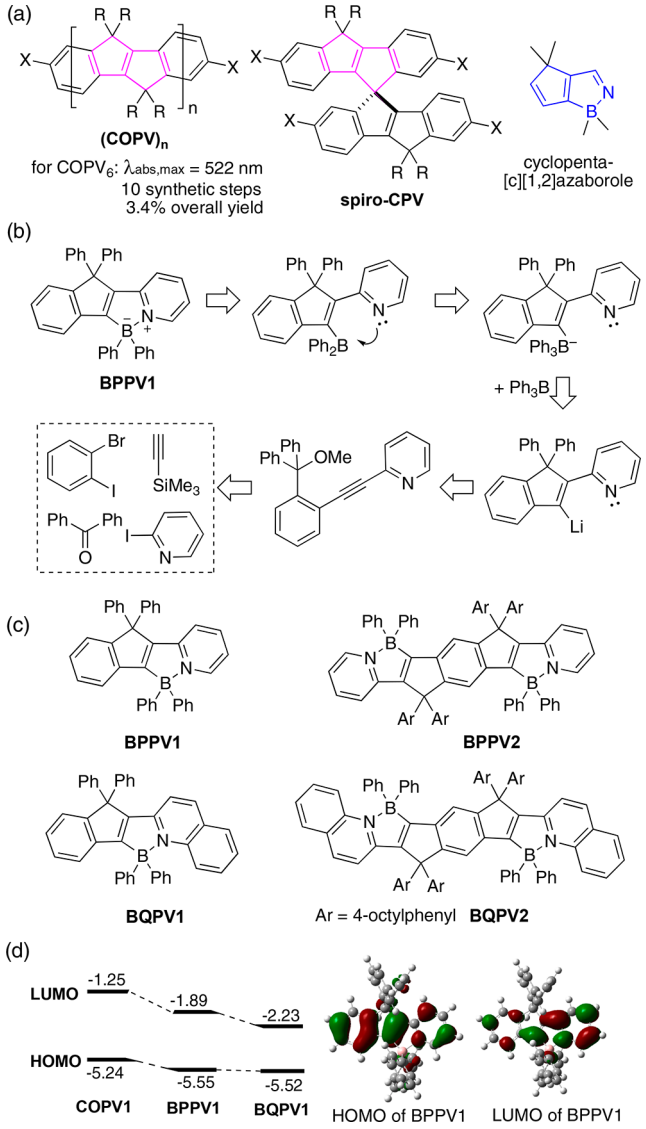

Figure 1. COPVs and their B/N-embedded congeners. (a) Structures of COPVs containing 1,4-dihydropentalene units (purple) and cyclopenta[*c*][1,2]azaborole unit (blue). (b) Retrosynthesis of **BPPV1** from commercially available materials. (c) Structures of B/N-doped *p*-arylenevinylenes. (d) Comparison of molecular orbital energetics of **COPV1**, **BPPV1**, and **BQPV1** using DFT and TD-DFT calculations at the B3LYP/6-31G (d, p) level.

small molecule to emit at a long wavelength (Figure 1d; see the Supporting Information for details).[14−16] Thus, we synthesized **BQPV2** in only five steps, which fluoresces at 540 nm with FLQY of 98%, from commercially available reagents. This molecule is much shorter in skeletal length at approximately half that of **COPV6** and is rigid, as attested by a very small Stokes shift value of 20 nm. Being photostable, **BQPV1** and **BQPV2** serve as viable cell-imaging dyes. We also showcase the ability of the emerging electron crystallographic technique,[17] with which we unambiguously determined the molecular structure and the crystal packing of **BPPV2**. This compound produced only a microcrystalline powder unsuitable for X-ray crystallographic analysis.

2. RESULTS AND DISCUSSION

2.1. Synthesis. The synthesis of **BPPV1** and **BQPV1** starts from commercially available 1-bromo-2-iodobenzene following a reported synthetic procedure developed for COPV synthesis to obtain acetylenes **1** and **2**.[4] Acetylene **2** was coupled with 2-iodopyridine or with 2-iodoquinoline using Sonogashira coupling to obtain **3** and **4**. Reductive cyclization of compounds **3** and **4** using lithium naphthalenide (LiNaph) at 0 °C formed 2-(pyridin-2-yl)- or 2-(quinolin-2-yl)-3-lithioindenes (cf. Figure 1b), which were trapped in situ with BPh_3, and a putative borate intermediate lost a phenyl group to obtain the target molecules, **BPPV1** and **BQPV1** (Scheme 1).

Scheme 1. Synthesis of BPPV1 and BQPV1

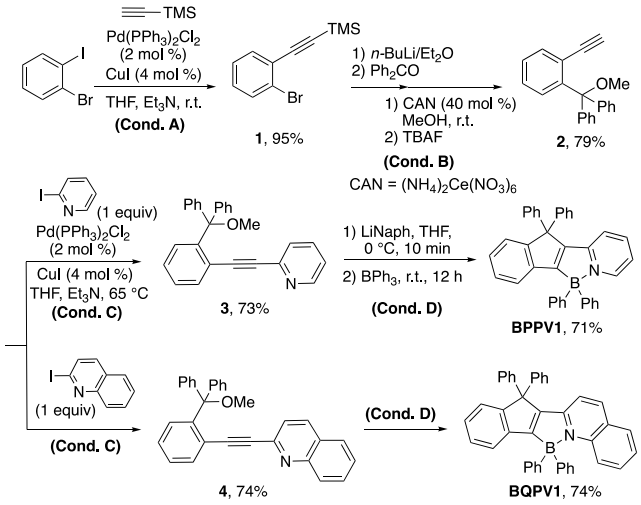

The similar synthetic sequence performed on two sides of 1,4-dibromo-2,5-diiodobenzene proceeded cleanly to give **BPPV2** and **BQPV2**, which attests to the efficiency of our B−N bond-forming strategy to obtain the rigid and flat conjugated systems (Scheme 2).

2.2. Electron Crystallographic Structural Analysis. Bearing four flexible *p*-octylphenyl side chains, **BPPV2** only produced powder crystals unsuitable for X-ray analysis (Figure 2a), and we decided to use electron crystallography (EC), an emerging technique in chemistry, suitable for structural

Scheme 2. Synthesis of BPPV2 and BQPV2

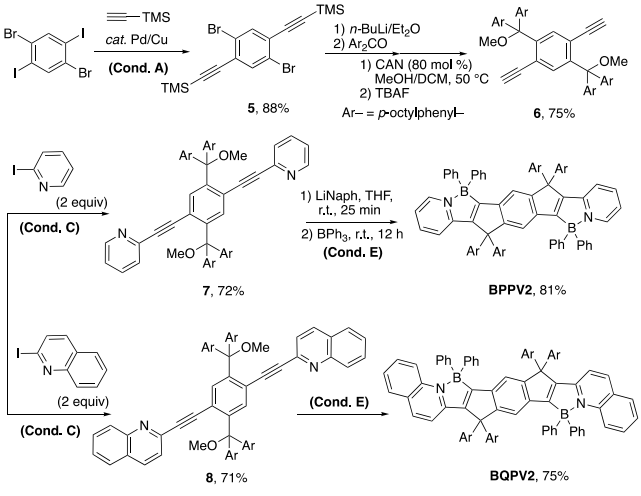

https://dx.doi.org/10.1021/jacs.0c10337
J. Am. Chem. Soc. 2020, 142, 18990−18996

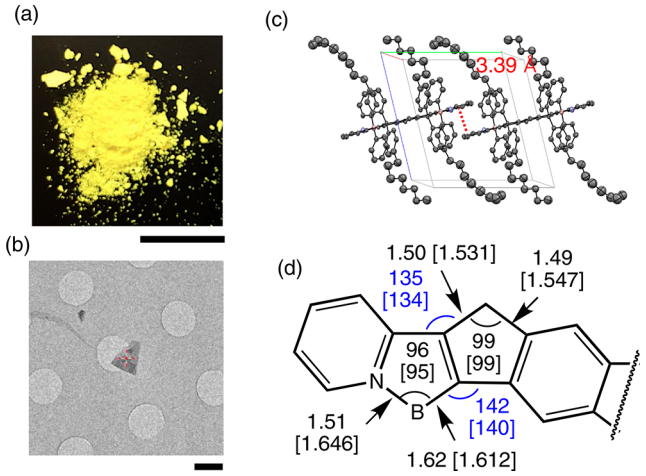

Figure 2. Microcrystal electron crystallographic analysis of **BPPV2** at 0.95 Å resolution at −180 °C. (a) A fine powder of an isolated sample. Scale bar 1 cm. (b) Low-magnification TEM image. Scale bar 1 μm. (c) Packing structure of **BPPV2** in a microcrystal. (d) Representative structural data (in Å and °; substituents are omitted) of **BPPV2** (EC). Data in brackets are calculated at the B3LYP/6-31G (d, p) level.

analysis of a microcrystalline powder[18,19] or of crystals with a low degree of crystalline order such as organic solid solutions.[6b] Microcrystals obtained by concentration of the eluate from silica gel chromatography (Figure 2a) were placed on an electron microscope grid coated with a 20 nm amorphous carbon film (see the Supporting Information for details, Figures S1 and S2). We analyzed the microcrystals one after another (Figure 2b) and from 29 data sets acquired an optimum three-dimensional molecular structure of **BPPV2** (see Figure S3) and the crystal packing shown in Figure 2c,d. One unit cell contains two molecules, each of which maintains 3.39 Å $\pi-\pi$ interaction with its neighbor on the terminal pyridine groups (Figure 2c). The ring strain of the cyclopenta-[*c*][1,2]azaborole system is highlighted by the extremely large bond angles around the tetrasubstituted olefin (Figure 2d, blue). In contrast to **BPPV2**, the molecules of **BBPV1** in the crystal are held together by CH$-\pi$ interactions at a distance of 2.95 Å instead of the $\pi-\pi$ interaction as shown by X-ray crystallographic analysis (see Supporting Information for details, Figure S4).

2.3. Photophysical Properties. The photophysical properties of B,N-*p*-arylenevinylenes as well as the parent COPV compounds are summarized in Figure 3 and Table 1, where we see significant bathochromic shifts by 42 and 83 nm in solution for **BPPV1** and **BQPV1**, respectively, relative to **COPV1** absorbing at 336 nm. We find a comparable shift for **BPPV2** (44 nm) and **BQPV2** (100 nm) over **COPV2**. Thus, the absorption and emission of **BQPV2** at 520 and 540 nm, respectively, are comparable to those of **COPV6** (522 and 536 nm).[4b] These molecules undergo light absorption with high molar extinction coefficients (ε_{max} = 1.40−5.45 × 10^4), and light emission with nearly quantitative FLQY (Φ_F = 0.96−1.00) and with a fluorescence lifetime reaching τ = 6.7 ns for **BPPV1** and **BQPV1** (see Figure S5). The Stokes shift (SS) values are generally small for B,N-*p*-arylenevinylenes. As found for COPVs, the rigid structure enhances the rate of radiative decay (k_r) relative to that of nonradiative decay (k_{nr}), which is negligibly small (Table 1). The SS values are very small for the

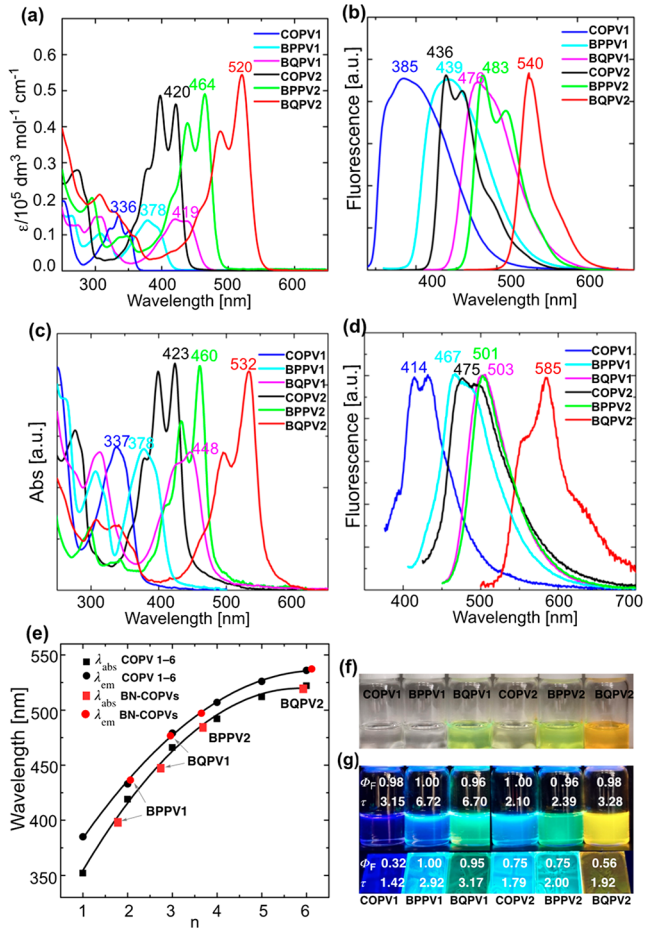

Figure 3. Photophysical properties of **BPPVs** and **BQPVs** in solution and thin film. (a) UV−vis absorption and (b) emission in DCM. (c) UV−vis absorption and (d) emission in film. (e) Comparison of absorption and emission wavelengths of **BPPVs** and **BQPVs** with **COPV1−6**. (f) Photographs of colors in DCM under room light. (g) Photographs in DCM and in film under 365 nm light irradiation.

C_2-symmetric **BPPV2** and **BQPV2** (19−20 nm), further attesting to the rigidity of the π-system.

Notably, the FLQY values of **BPPV1** and **BQPV1** are nearly quantitative in their drop-cast films (Φ_F = 1.00 and 0.95 in a film for **BPPV1** and **BQPV1**, respectively) as they are nearly so in solution (Φ_F = 1.00 and 0.96). Other absorption/emission profiles in the film state are summarized on the right side of Table 1. The data in the film state compare favorably with their solution counterparts, reflecting the very small intermolecular interactions found for the crystal of **BPPV1** (see Figure S4). On the other hand, for the doubly cyclized congeners, the FLQY of **BPPV2** and **BQPV2** decreased from Φ_F = 0.96 and 0.98 in solution to 0.75 and 0.56 in film, respectively, which we may ascribe to $\pi-\pi$ interactions (3.39 Å, Figure 2c) of the terminal aromatic rings as found in the **BPPV2** crystal (Figure 2c). The observed bathochromic shift of **BQPV1** and **BQPV2** upon going from solution to film may also stem from this $\pi-\pi$ interaction.

The electrochemical properties were studied using cyclic voltammetry (CV) and differential pulse voltammetry (DPV) in dichloromethane (DCM). Unlike **COPV1** (0.86 V) and **COPV2** (0.53 V), which undergo reversible oxidations, **BPPV1** and **BQPV1** undergo a single irreversible oxidation at 0.87 and 0.90 V, respectively. In contrast, the doubly B/N-

https://dx.doi.org/10.1021/jacs.0c10337
J. Am. Chem. Soc. 2020, 142, 18990−18996

Table 1. Photophysical Properties of BPPVs, BQPVs, and COPVs

	DCM solution								neat film			
	λ_{abs} (nm)	ε_{max} $(10^4)^a$	λ_{em} (nm)	SS[b] [cm^{-1}, (nm)]	$\Phi_F{}^c$	τ $(ns)^d$	k_r $(10^8\ s^{-1})^e$	k_{nr} $(10^8\ s^{-1})^f$	λ_{abs} (nm)	λ_{em} (nm)	$\Phi_F{}^g$	τ $(ns)^h$
COPV1	336, 352	1.53	385	2435 (33)	0.98	3.15	3.11	0.06	337	414, 432	0.32	1.42
BPPV1	378, 393	1.40	439	2666 (46)	1.00	6.72	1.49	–	378	467	1.00	2.92
BQPV1	419, 439	1.44	476	1770 (37)	0.96	6.70	1.43	0.06	448	503	0.95	3.17
COPV2	397, 420	4.84	436, 457	874 (16)	1.00	2.10	4.76	–	400, 423	475, 497	0.75	1.79
BPPV2	439, 464	4.88	483, 511	845 (19)	0.96	2.39	4.02	0.16	434, 460	501	0.75	2.00
BQPV2	488, 520	5.45	540	712 (20)	0.98	3.28	2.99	0.06	497, 532	557, 585	0.56	1.92

[a]Extinction coefficients (L mol^{-1} cm^{-1}) for the most intense absorption band. [b]Stokes shift. [c]Fluorescence quantum yield determined using an absolute method. [d]Fluorescence lifetime measured with the time-correlated single-photon counting operation mode. [e]Radiative rate constants were calculated from $k_r = \Phi_F/\tau$. [f]Nonradiative rate constants were calculated from $k_{nr} = (1 - \Phi_F)/\tau$. [g]Fluorescence quantum yield determined using an absolute method in drop-cast film. [h]Uniform film.

Table 2. Electrochemical Properties and Calculated HOMO−LUMO Energies of COPVs, BPPVs, and BQPVs

	IP $(eV)^a$	$E_{pa/2}$ (V vs Fc/Fc^+)[b]	OBG $(eV)^c$	E_H $(eV)^d$	E_L $(eV)^e$	E_H $(eV)^f$	E_L $(eV)^g$	$\Delta E_{H-L,\ calc}$ $(eV)^h$
COPV1	5.93	0.86	3.35	−5.66	−2.31	−5.24	−1.25	3.99
BPPV1	6.03	0.87	2.95	−5.67	−2.72	−5.55	−1.89	3.66
BQPV1	6.05	0.90	2.63	−5.70	−2.97	−5.52	−2.23	3.29
COPV2	5.74	0.53	2.77	−5.33	−2.56	−4.83	−1.56	3.27
BPPV2	5.90	0.63	2.51	−5.43	−2.92	−5.17	−2.14	3.03
BQPV2	5.93	0.66	2.23	−5.45	−3.22	−5.16	−2.42	2.74

[a]IP measured using PYS in a film on the ITO surface. [b]Oxidation potential (0.5 mM in DCM with 0.1 M Bu_4NPF_6 electrolyte). $E_{1/2}$ value for COPVs. [c]Optical band gap determined from the offset of absorption spectra in DCM. [d]HOMO level determined from oxidation potential. [e]LUMO level determined from oxidation potential and optical band gap. [f]Calculated HOMO level. [g]Calculated LUMO level. [h]HOMO−LUMO gap calculated at the B3LYP/6-31G(d, p) level of theory.

doped **BPPV2** and **BQPV2** undergo two irreversible oxidations at 0.63 and 0.84 V for **BPPV2** and 0.66 and 0.90 V for **BQPV2** (Table 2, Figure S6, see the Supporting Information). The LUMOs of **BPPV1** and **BPPV2** are much lower than those of **COPV1** and **COPV2**. The ionization potentials (IP) were determined using photoelectron yield spectroscopy (PYS) in the thin-film state to be 6.03 eV (**BPPV1**) and 5.90 eV (**BPPV2**), values slightly larger than those of **COPVs**. The IP data agree in their trend with the HOMO energies estimated using DPV measurements (Table 2, Figure S7, see the Supporting Information). The optical band gaps of **BPPV1** (2.95 eV) and **BPPV2** (2.51 eV) are smaller than those of **COPV1** (3.35 eV) and **COPV2** (2.77 eV).

Density functional theory (DFT) and TD-DFT calculations provide further insights into the electronic transition of the B,N-*p*-arylenevinylenes (Figures S8 and S9 and Table S2, see the Supporting Information for details). The incorporation of BN units does not significantly change the rigidity and flatness of the molecular geometries. The main absorption band is assignable to S_0-S_1 transitions from a HOMO → LUMO one-electron excitation. The HOMO orbital is localized primarily on the indenyl fragment and less on the pyridyl or quinolinyl moiety, while the LUMO is localized largely on the pyridyl and quinolinyl moieties.

2.4. Photostability. BPPVs and BQPVs showed high photostability similar to that of **COPVs** (Figure 4a). Notably, **BQPV2** retained >95% of the initial fluorescence intensity under continuous excitation by a 300 W xenon lamp for 60 min, and so did the other congeners (Figure 4a). The new B/N-doped chromophores survive far better under intercellular conditions than a commercial BODIPY 493/503 (Figure 4b) and suggest their applications for live-cell imaging.[20] Confocal fluorescence images of human mammary cancer MCF-7 cells

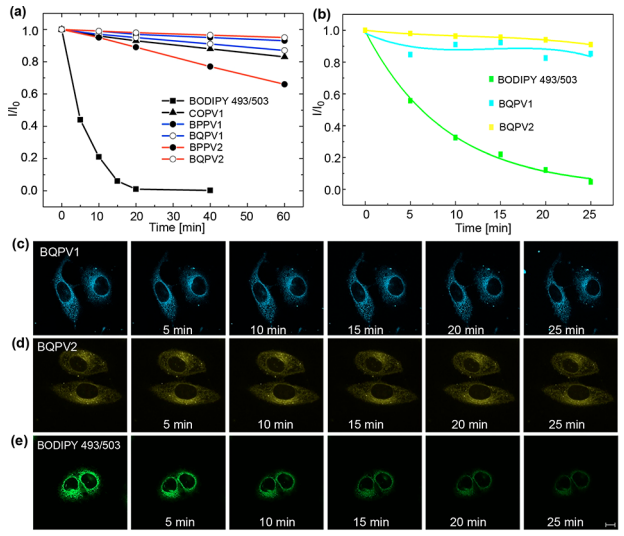

Figure 4. Photostability and cell-imaging application. (a) Photostability of **COPV1**, BPPVs, BQPVs, and BODIPY 493/503 in THF. Photostability was determined by measuring the change in fluorescent intensity (I/I_0) at a maximum band under illumination with a 300 W xenon lamp (luminous intensity: 1450 cd). (b) Plots of normalized intracellular fluorescence intensity. Normalization was carried out against the initial fluorescence intensity. Image comparison of photostability of (c) **BQPV1**, (d) **BQPV2**, and (e) BODIPY 493/503 in MCF-7 cells using LSM800 with a Plan-Apochromat 63×/1.40 oil DIC M27 lens (Zeiss). **BQPV1** was excited at 405 nm with a violet laser diode (5 mW), and **BQPV2** and BODIPY 493/503 were excited at 488 nm with an argon-ion laser (10 mW). Scale bar = 10 μm.

in Figure 4c−e show the comparison among **BQPV1**, **BQPV2**, and BODIPY 493/503 (Supporting Information for details).[21] **BQPV1** and **BQPV2** remained virtually unchanged in 25 min

https://dx.doi.org/10.1021/jacs.0c10337
J. Am. Chem. Soc. 2020, 142, 18990−18996

under continuous irradiation, whereas BODIPY 493/503 lost much of the fluorescence after 25 min (Figure 4c–e). Interestingly, the cells stained using BQPVs showed a staining pattern of fluorescent cell images different from those with BODIPY 493/503, which will be a subject of further investigation. These preliminary experiments suggested **BQPV2** as a staining dye for long-term visualization of biological events.

3. CONCLUSION

In summary, we document here a short-step synthesis and properties of a series of B,N-*p*-arylenevinylenes, which feature excellent FLQY and photostability. Microcrystal EC analysis on a powder sample unsuitable for X-ray crystallography revealed the molecular structure of **BPPV2** and its packing in the solid state. **BQPV2** showed a Φ_F = 98% and absorption at 520 nm, which are similar to those recorded for **COPV6**, a molecule much larger in conjugation length and hence requiring more synthetic effort. The B,N-*p*-arylenevinylenes resist photobleaching and serve as lipophilic fluorescent dyes for long-term live-cell imaging with staining patterns different from that of BODIPY 493/503 dyes, suggesting potential application for various biological imaging.

■ ASSOCIATED CONTENT

Supporting Information

The Supporting Information is available free of charge at https://pubs.acs.org/doi/10.1021/jacs.0c10337.

Materials and methods; experimental procedures; additional spectra; characterization data; TD-DFT calculations (PDF)

(CIF)

(CIF)

■ AUTHOR INFORMATION

Corresponding Authors

Rui Shang − *Department of Chemistry, School of Science, The University of Tokyo, Tokyo 113-0033, Japan;* orcid.org/0000-0002-2513-2064; Email: rui@chem.s.u-tokyo.ac.jp

Eiichi Nakamura − *Department of Chemistry, School of Science, The University of Tokyo, Tokyo 113-0033, Japan;* orcid.org/0000-0002-4192-1741; Email: nakamura@chem.s.u-tokyo.ac.jp

Authors

Hua Lu − *Department of Chemistry, School of Science, The University of Tokyo, Tokyo 113-0033, Japan; Key Laboratory of Organosilicon Chemistry and Material Technology, Ministry of Education, Hangzhou Normal University, Hangzhou 311121, China;* orcid.org/0000-0003-4225-9101

Takayuki Nakamuro − *Department of Chemistry, School of Science, The University of Tokyo, Tokyo 113-0033, Japan*

Keitaro Yamashita − *Department of Biological Sciences, Graduate School of Science, The University of Tokyo, Tokyo 113-0033, Japan;* orcid.org/0000-0002-5442-7582

Haruaki Yanagisawa − *Department of Cell Biology and Anatomy, Graduate School of Medicine, The University of Tokyo, Tokyo 113-0033, Japan*

Osamu Nureki − *Department of Biological Sciences, Graduate School of Science, The University of Tokyo, Tokyo 113-0033, Japan*

Masahide Kikkawa − *Department of Cell Biology and Anatomy, Graduate School of Medicine, The University of Tokyo, Tokyo 113-0033, Japan*

Han Gao − *State Key Laboratory of Natural Medicines, School of Traditional Chinese Pharmacy, China Pharmaceutical University, Nanjing 211198, P.R. China*

Jiangwei Tian − *State Key Laboratory of Natural Medicines, School of Traditional Chinese Pharmacy, China Pharmaceutical University, Nanjing 211198, P.R. China;* orcid.org/0000-0003-1018-4694

Complete contact information is available at: https://pubs.acs.org/10.1021/jacs.0c10337

Notes

The authors declare no competing financial interest.

■ ACKNOWLEDGMENTS

This research is supported by MEXT KAKENHI grant number 19H05459 (to E.N.) and JSPS KAKENHI grant number 19K15555 (to R.S.). We thank Mitsubishi Chemical Corporation for partial financial support. K.Y. thanks JSPS KAKENHI for financial support (20K15729). This research was also supported by the Platform Project for Supporting Drug Discovery and Life Science Research (Basis for Supporting Innovative Drug Discovery and Life Science Research (BINDS)) from AMED under grant number JP19am0101115 (*support number 2031*).

■ REFERENCES

(1) Shirakawa, H. Nobel Lecture: The discovery of polyacetylene film-the dawning of an era of conducting polymers. *Rev. Mod. Phys.* **2001**, *73*, 713–718.

(2) (a) Ito, T.; Shirakawa, H.; Ikeda, S. Simultaneous polymerization and formation of polyacetylene film on the surface of concentrated soluble Ziegler-type catalyst solution. *J. Polym. Sci., Polym. Chem.* **1974**, *12*, 11–20. (b) Shirakawa, H.; Louis, E. J.; MacDiarmid, A. G.; Chiang, C. K.; Heeger, A. J. Synthesis of electrically conducting organic polymers: halogen derivatives of polyacetylene, (CH)x. *J. Chem. Soc., Chem. Commun.* **1977**, *16*, 578–580. (c) Chiang, C. K.; Fincher, C. R.; Park, Y. W.; Heeger, A. J.; Shirakawa, H.; Louis, E. J.; Gau, S. C.; MacDiarmid, A. G. Electrical Conductivity in Doped Polyacetylene. *Phys. Rev. Lett.* **1977**, *39*, 1098–1101.

(3) (a) Granier, T.; Thomas, E. L.; Gagnon, D. R.; Karasz, F. E.; Lenz, R. W. Structure investigation of poly(*p*-phenylene vinylene). *J. Polym. Sci., Part B: Polym. Phys.* **1986**, *24*, 2793–2804. (c) Burroughes, J. H.; Bradley, D. D. C.; Brown, A. R.; Marks, R. N.; MacKay, K.; Friend, R. H.; Burns, P. L.; Holmes, A. B. Light-emitting diodes based on conjugated polymers. *Nature* **1990**, *347*, 539–541.

(4) (a) Zhu, X.; Mitsui, C.; Tsuji, H.; Nakamura, E. Modular Synthesis of 1H-Indenes, Dihydro-*s*-Indacene, and Diindenoindacene—a Carbon-Bridged p-Phenylenevinylene Congener. *J. Am. Chem. Soc.* **2009**, *131*, 13596–13597. (b) Zhu, X.; Tsuji, H.; López Navarrete, J. T.; Casado, J.; Nakamura, E. Carbon-Bridged Oligo(phenylenevinylene)s: Stable π-Systems with High Responsiveness to Doping and Excitation. *J. Am. Chem. Soc.* **2012**, *134*, 19254–19259.

(5) Tsuji, H.; Nakamura, E. Carbon-Bridged Oligo(phenylene vinylene)s: A de Novo Designed, Flat, Rigid, and Stable π-Conjugated System. *Acc. Chem. Res.* **2019**, *52*, 2939–2949.

(6) (a) Hamada, H.; Itabashi, Y.; Shang, R.; Nakamura, E. Axially Chiral Spiro-Conjugated Carbon-Bridged *p*-Phenylenevinylene Congeners: Synthetic Design and Materials Properties. *J. Am. Chem. Soc.* **2020**, *142*, 2059–2067. (b) Hamada, H.; Nakamuro, T.; Yamashita, K.; Yanagisawa, H.; Nureki, O.; Kikkawa, M.; Harano, K.; Shang, R.; Nakamura, E. Spiro-Conjugated Carbon/Heteroatom-Bridged *p*-Phenylenevinylenes: Synthesis, Properties, and Microcrystal Electron

Crystallographic Analysis of Racemic Solid Solutions. *Bull. Chem. Soc. Jpn.* **2020**, *93*, 776−782.
(7) (a) Sukegawa, J.; Schubert, C.; Zhu, X.; Tsuji, H.; Guldi, D. M.; Nakamura, E. Electron transfer through rigid organic molecular wires enhanced by electronic and electron-vibration coupling. *Nat. Chem.* **2014**, *6*, 899−905. (b) Burrezo, P. M.; Zhu, X.; Zhu, S. F.; Yan, Q.; López Navarrete, J. T.; Tsuji, H.; Nakamura, E.; Casado, J. Planarization, Fusion, and Strain of Carbon-Bridged Phenylenevinylene Oligomers Enhance π-Electron and Charge Conjugation: A Dissectional Vibrational Raman Study. *J. Am. Chem. Soc.* **2015**, *137*, 3834−3843. (c) Yan, Q.; Guo, Y.; Ichimura, A.; Tsuji, H.; Nakamura, E. Three-Dimensionally Homoconjugated Carbon-Bridged Oligophenylenevinylene for Perovskite Solar Cells. *J. Am. Chem. Soc.* **2016**, *138*, 10897−10904.
(8) (a) Burrezo, P. M.; Lin, N. T.; Nakabayashi, K.; Ohkoshi, S.-i.; Calzado, E. M.; Boj, P. G.; Díaz García, M. A.; Franco, C.; Rovira, C.; Veciana, J.; Moos, M.; Lambert, C.; López Navarrete, J. T.; Tsuji, H.; Nakamura, E.; Casado, J. Bis(aminoaryl) Carbon-Bridged Oligo(phenylenevinylene)s Expand the Limits of Electronic Couplings. *Angew. Chem., Int. Ed.* **2017**, *56*, 2898−2902. (b) Nishioka, H.; Tsuji, H.; Nakamura, E. Homo- and Copolymers Based on Carbon-Bridged Oligo(*p*-phenylenevinylene)s for Efficient Fluorescence over the Entire Visible Region. *Macromolecules* **2018**, *51*, 2961−2968. (c) Morales-Vidal, M.; Boj, P. G.; Villalvilla, J. M.; Quintana, J. A.; Yan, Q.; Lin, N. T.; Zhu, X.; Ruangsupapichat, N.; Casado, J.; Tsuji, H.; Nakamura, E.; Díaz-García, M. A. Carbon-bridged oligo(p-phenylenevinylene)s for photostable and broadly tunable, solution-processable thin film organic lasers. *Nat. Commun.* **2015**, *6*, 8458.
(9) (a) Zhu, X.; Tsuji, H.; Nakabayashi, K.; Ohkoshi, S.; Nakamura, E. Air- and Heat-Stable Planar Tri-*p*-quinodimethane with Distinct Biradical Characteristics. *J. Am. Chem. Soc.* **2011**, *133*, 16342−16345. (b) Zhu, X.; Tsuji, H.; Yella, A.; Chauvin, A. S.; Grätzel, M.; Nakamura, E. New sensitizers for dye-sensitized solar cells featuring a carbon-bridged phenylenevinylene. *Chem. Commun.* **2013**, *49*, 582−584.
(10) (a) Dewar, M. J. S.; Dietz, R. New heteroaromatic compounds. Part III. 2,1-Borazaro-naphthalene (1,2-dihydro-1-aza-2-boranaphthalene). *J. Chem. Soc.* **1959**, 2728−2730. (b) Jäkle, F.; Priermeier, T.; Wagner, M. Synthesis, Structure, and Dynamic Behavior of ansa-Ferrocenes with Pyrazabole Bridges. *Organometallics* **1996**, *15*, 2033−2040. (c) Jäkle, F.; Priermeier, T.; Wagner, M. Novel ansa-ferrocenes with o-phenylene-type bridges by B-N adduct formation. *J. Chem. Soc., Chem. Commun.* **1995**, 1765−1766. (d) Grosche, M.; Herdtweck, E.; Peters, F.; Wagner, M. Boron-Nitrogen Coordination Polymers Bearing Ferrocene in the Main Chain. *Organometallics* **1999**, *18*, 4669−4672. (e) Fontani, M.; Peters, F.; Scherer, W.; Wachter, W.; Wagner, M.; Zanello, P. Adducts of Ferrocenylboranes and Pyridine Bases: Generation of Charge-Transfer Complexes and Reversible Coordination Polymers. *Eur. J. Inorg. Chem.* **1998**, 1453−1465.
(11) (a) Ci, L.; Song, L.; Jin, C.; Jariwala, D.; Wu, D.; Li, Y.; Srivastava, A.; Wang, Z. F.; Storr, K.; Balicas, L.; Liu, F.; Ajayan, P. M. Atomic layers of hybridized boron nitride and graphene domains. *Nat. Mater.* **2010**, *9*, 430−435. (b) Hatakeyama, T.; Hashimoto, S.; Seki, S.; Nakamura, M. Synthesis of BN-Fused Polycyclic Aromatics via Tandem Intramolecular Electrophilic Arene Borylation. *J. Am. Chem. Soc.* **2011**, *133*, 18614−18617. (c) Nakatsuka, S.; Yasuda, N.; Hatakeyama, T. Four-Step Synthesis of B2N2-Embedded Corannulene. *J. Am. Chem. Soc.* **2018**, *140*, 13562−13565. (d) Lu, H.; Mack, J.; Yang, Y.; Shen, Z. Structural modification strategies for the rational design of red/NIR region BODIPYs. *Chem. Soc. Rev.* **2014**, *43*, 4778−4823.
(12) (a) Wang, X. Y.; Narita, A.; Feng, X.; Müllen, K. B2N2-Dibenzo[a,e]pentalenes: Effect of the BN Orientation Pattern on Antiaromaticity and Optoelectronic Properties. *J. Am. Chem. Soc.* **2015**, *137*, 7668−7671. (b) Wang, X. Y.; Wang, J. Y.; Pei, J. BN Heterosuperbenzenes: Synthesis and Properties. *Chem. - Eur. J.* **2015**, *21*, 3528−3539. (c) Jaska, C. A.; Emslie, D. J. H.; Bosdet, M. J. D.; Piers, W. E.; Sorensen, T. S.; Parvez, M. Triphenylene Analogues with B2N2C2 Cores: Synthesis, Structure, Redox Behavior, and Photophysical Properties. *J. Am. Chem. Soc.* **2006**, *128*, 10885−10896.
(13) (a) Abengózar, A.; García-García, P.; Sucunza, D.; Sampedro, D.; Pérez-Redondo, A.; Vaquero, J. J. Synthesis, Functionalization, and Optical Properties of 1,2-Dihydro-1-aza-2-boraphenanthrene and Several Highly Fluorescent Derivatives. *Org. Lett.* **2019**, *21*, 2550−2554. (b) Kaehler, T.; Bolte, M.; Lerner, H.-W.; Wagner, M. Introducing Perylene as a New Member to the Azaborine Family. *Angew. Chem., Int. Ed.* **2019**, *58*, 11379−11384. (c) McConnell, C. R.; Haeffner, F.; Baggett, A. W.; Liu, S.-Y. 1,2-Azaborine's Distinct Electronic Structure Unlocks Two New Regioisomeric Building Blocks via Resolution Chemistry. *J. Am. Chem. Soc.* **2019**, *141*, 9072−9078.
(14) (a) Wakamiya, A.; Taniguchi, T.; Yamaguchi, S. Intramolecular B-N Coordination as a Scaffold for Electron-Transporting Materials: Synthesis and Properties of Boryl-Substituted Thienylthiazoles. *Angew. Chem., Int. Ed.* **2006**, *45*, 3170−3173. (b) Nakamura, T.; Furukawa, S.; Nakamura, E. Benzodipyrrole-based Donor-Acceptor-type Boron Complexes as Tunable Near-infrared-Absorbing Materials. *Chem. - Asian J.* **2016**, *11*, 2016−2020.
(15) (a) Liu, K.; Lalancette, R. A.; Jäkle, F. Tuning the Structure and Electronic Properties of B-N Fused Dipyridylanthracene and Implications on the Self-Sensitized Reactivity with Singlet Oxygen. *J. Am. Chem. Soc.* **2019**, *141*, 7453−7462. (b) Wang, S.; Yuan, K.; Hu, M.-F.; Wang, X.; Peng, T.; Wang, N.; Li, Q.-S. Cleavage of Unstrained C-C Bonds in Acenes by Boron and Light: Transformation of Naphthalene into Benzoborepin. *Angew. Chem., Int. Ed.* **2018**, *57*, 1073−1077. (c) Shen, C.; Srebro-Hooper, M.; Jean, M.; Vanthuyne, N.; Toupet, L.; Williams, J. A. G.; Torres, A. R.; Riives, A. J.; Muller, G.; Autschbach, J.; Crassous, J. Synthesis and Chiroptical Properties of Hexa-, Octa-, and Deca-azaborahelicenes: Influence of Helicene Size and of the Number of Boron Atoms. *Chem. - Eur. J.* **2017**, *23*, 407−418.
(16) (a) Min, Y.; Dou, C.; Liu, D.; Dong, H.; Liu, J. Quadruply B←N-Fused Dibenzo-azaacene with High Electron Affinity and High Electron Mobility. *J. Am. Chem. Soc.* **2019**, *141*, 17015−17021. (b) Farrell, J. M.; Mützel, C.; Bialas, D.; Rudolf, M.; Menekse, K.; Krause, A. M.; Stolte, M.; Würthner, F. Tunable Low-LUMO Boron-Doped Polycyclic Aromatic Hydrocarbons by General One-Pot C-H Borylations. *J. Am. Chem. Soc.* **2019**, *141*, 9096−9104.
(17) Palatinus, L.; Brázda, P.; Boullay, P.; Perez, O.; Klementová, M.; Petit, S.; Eigner, V.; Zaarour, M.; Mintova, S. Hydrogen positions in single nanocrystals revealed by electron diffraction. *Science* **2017**, *355*, 166−169.
(18) (a) Kolb, U.; Gorelik, T. E.; Mugnaioli, E.; Stewart, A. Structural Characterization of Organics Using Manual and Automated Electron Diffraction. *Polym. Rev.* **2010**, *50*, 385−409. (b) Gruene, T.; Wennmacher, J. T. C.; Zaubitzer, C.; Holstein, J. J.; Heidler, J.; Fecteau-Lefebvre, A.; De Carlo, S.; Müller, E.; Goldie, K. N.; Regeni, I.; Li, T.; Santiso-Quinones, G.; Steinfeld, G.; Handschin, S.; van Genderen, E.; van Bokhoven, J. A.; Clever, G. H.; Pantelic, R. Rapid Structure Determination of Microcrystalline Molecular Compounds Using Electron Diffraction. *Angew. Chem., Int. Ed.* **2018**, *57*, 16313−16317. (c) Justel, D.; Friesecke, G.; James, R. D. Bragg-von Laue diffraction generalized to twisted X-rays. *Acta Crystallogr., Sect. A: Found. Adv.* **2016**, *72*, 190−196.
(19) (a) Jones, C. G.; Martynowycz, M. W.; Hattne, J.; Fulton, T. J.; Stoltz, B. M.; Rodriguez, J. A.; Nelson, H. M.; Gonen, T. The CryoEM Method MicroED as a Powerful Tool for Small Molecule Structure Determination. *ACS Cent. Sci.* **2018**, *4*, 1587−1592. (b) Gemmi, M.; Mugnaioli, E.; Gorelik, T. E.; Kolb, U.; Palatinus, L.; Boullay, P.; Hovmöller, S.; Abrahams, J. P. 3D Electron Diffraction: The Nanocrystallography Revolution. *ACS Cent. Sci.* **2019**, *5*, 1315−1329. (c) Guzmán-Afonso, C.; Hong, Y.; Colaux, H.; Iijima, H.; Saitow, A.; Fukumura, T.; Aoyama, Y.; Motoki, S.; Oikawa, T.; Yamazaki, T.; Yonekura, K.; Nishiyama, Y. Understanding hydrogen-bonding structures of molecular crystals via electron and NMR nanocrystallography. *Nat. Commun.* **2019**, *10*, 3537.

https://dx.doi.org/10.1021/jacs.0c10337
J. Am. Chem. Soc. 2020, 142, 18990−18996

(20) Wang, C.; Taki, M.; Sato, Y.; Fukazawa, A.; Higashiyama, T.; Yamaguchi, S. Super-Photostable Phosphole-Based Dye for Multiple-Acquisition Stimulated Emission Depletion Imaging. *J. Am. Chem. Soc.* **2017**, *139*, 10374−10351.
(21) (a) Loudet, A.; Burgess, K. BODIPY dyes and their derivatives: synthesis spectroscopic properties. *Chem. Rev.* **2007**, *107*, 4891−4932. (b) Kowada, T.; Maeda, H.; Kikuchi, K. BODIPY-based probes for the fluorescence imaging of biomolecules in living cells. *Chem. Soc. Rev.* **2015**, *44*, 4953−4972.

https://dx.doi.org/10.1021/jacs.0c10337
J. Am. Chem. Soc. 2020, 142, 18990−18996